Advantages and Limitations of Active Phase Silanization in PVDF Composites: Focus on Electrical Properties and Energy Harvesting Potential

M. Vijatovic Petrovic[1*], F. Craciun[2], F. Cordero[2], E. Mercadelli[3], N. Ilic[4], Z. Despotovic[5], J. Bobic[1], A. Dzunuzovic[1], C. Galassi[3], P. Stagnaro[6], G. Canu[7], M.T. Buscaglia[7], E. Brunengo[6]

[1] University of Belgrade, Institute for Multidisciplinary Research, Kneza Viseslava 1, 11 000 Belgrade, Serbia
[2]CNR-ISM, Istituto di Struttura della Materia, Area della Ricerca di Tor Vergata, Via del Fosso del Cavaliere, 100, I-00133, Rome, Italy
[3]CNR- ISSMC - Istituto di Scienza, Tecnologia e Sostenibilità per lo Sviluppo dei Materiali Ceramici; Via Granarolo 64, I-48018 Faenza, Italy
[4]Vinča Institute of Nuclear Sciences, National Institute of the Republic of Serbia, University of Belgrade, Mike Petrovića Alasa 12-14, 11000 Belgrade, Serbia
[5]Institute Mihajlo Pupin, University of Belgrade, Volgina 15, 11000 Belgrade, Serbia
[6] CNR-SCITEC, Istituto di Scienze e Tecnologie Chimiche "Giulio Natta", Via de Marini 6, I-16149, Genoa, Italy
[7] CNR-ICMATE, Istituto di Chimica della Materia Condensata e di Tecnologie per l'Energia, Via de Marini 6, I-16149, Genoa, Italy

Abstract

In order to further improve the performance of $0.94[(Bi_{0.5}Na_{0.5})TiO_3]$-$0.06BaTiO_3$/polyvinylidene fluoride (NBT-BT/PVDF) flexible composite films prepared by the hot-pressing method, the effect of surface modification of the NBT-BT particles on the structure and properties of the films was investigated. Two coupling agents, namely, (3-aminopropyl)triethoxysilane (APTES) and dodecyl triethoxysilane (DDTES) were added to enhance dispersion and interfacial adhesion of the active phase powder with the polymer matrix. The highest amount of the electroactive PVDF β- phase was formed in APTES-modified samples while in DDTES samples mainly γ- phase was formed as shown by FTIR analysis. DSC measurements indicated that the addition of filler particles reduced the total crystallinity degree of the PVDF. Dielectric permittivity values as well as dielectric losses decreased for silanized samples due to reduced tension at the interface between particles and polymer. Strong intermolecular interaction between the PVDF chains and the APTES-modified particles led to enhanced breakdown strength of these samples. The highest level of agglomeration in the DDTES-modified samples induced the deterioration of ferroelectric properties. The highest voltage output of ~ 15 V and 225 μW of power was obtained for the APTES-modified harvester, evidencing their potential for energy harvesting applications.

* Corresponding author, +381112085039, e-mail: miravijat@yahoo.com

Highlights

- Surface of NBT-BT particles was successfully modified by the silanization method.
- NBT-BT-PVDF flexible lead-free composite films were prepared by hot pressing.
- APTES coupling agent enabled the transformation of PVDF α-phase into electro-active β.
- APTES-modified samples showed the highest breakdown strength.
- Notable properties for energy harvesting application found, up to 225 μW of generated power.

Keywords: polymer composite films, dielectric properties, piezoelectricity, energy harvesting

1. Introduction

Various forms of mechanical energy in the surrounding environment offer a valuable resource for piezoelectric energy harvesting. This technology enables the conversion of mechanical stress into electrical energy. The applications for this innovative approach can be wide-ranging, particularly in low-power devices that require autonomous energy sources. Piezoelectric energy harvesting has the potential to improve areas where traditional power sources like batteries and cables face limitations. Different kinds of sensors, alarms, lights, and other low-power devices can now operate in remote where conventional power solutions are either expensive or impractical. This technology opens up opportunities for placing sensors and measurement instruments in previously inaccessible locations, thereby enhancing our ability to collect data and monitor systems in a more sustainable and cost-effective manner [1-6].

Till now, lead-based materials have shown the best piezoelectric performance, finding widespread commercial applications. Nevertheless, these materials are confronted with a critical issue – environmental incompatibility. The demand for their replacement is unavoidable in the years to come, driven by concerns over their ecological impact. Among lead-free piezoelectric ceramic materials, NBT-based solution has become one of the most widely investigated piezoelectric systems in the last decade for its interesting energy storage properties [7-12]. Meanwhile, ceramic piezo-generators, while effective, have traditionally been rigid and prone to breakage. Addressing this challenge is crucial for expanding their utility. To create a piezoelectric energy harvester capable of conforming to various shapes and surfaces, it is imperative to introduce a flexible component into the material composition. This need for flexibility leads to innovative solutions in the field of materials science. Researchers and engineers are actively exploring ways to enhance the flexibility of piezoelectric materials, aiming to maintain or even improve their energy-harvesting capabilities while making them adaptable to diverse applications. Polymers like poly(vinylidene fluoride) (PVDF) and its co-polymers, cellulose, and derivatives, polyamides (PA), poly(lactic acid) (PLA), etc. are well-known polymers that have been used as a matrix in the preparations of ceramics/polymer composites materials [9-15]. The potential application as energy harvesters of in-house developed composites $0.94[(Bi_{0.5}Na_{0.5})TiO_3]$-$0.06BaTiO_3$ (NBT-BT) in PVDF matrix was already shown in the previous papers [11, 12].

The difference in dielectric permittivity values between the NBT-BT ceramic, ~ 2000, and PVDF polymer, ~10 is quite large [9]. When incorporating filler particles into a polymer matrix, several challenges can arise. These challenges include the agglomeration of particles, an uneven distribution of ceramic filler within the matrix, the formation of defects and voids, and subsequent deterioration of the mechanical and electrical properties of the composite (as documented in references [11,12]. It is essential to address these issues to achieve a high-quality composite material. Numerous researchers have emphasized the critical importance of the interface between the active phase (filler) and the polymer matrix in ensuring a homogeneous composite [16-20]. To promote the even distribution and dispersion of inorganic fillers within a polymer matrix while enhancing adhesion between the filler and the matrix, a technique involving the coating of filler particles with a thin layer of silane coupling agents or polymers has been introduced [18, 21-23].

The silanization process, particularly relevant when there is a substantial difference in dielectric permittivity between the active phase powder and the polymer matrix, offers an effective solution. It involves applying silane coupling agents to the surface of ceramic particles, facilitating improved dispersion and interfacial adhesion with the polymer matrix [21-25]. This technique plays a crucial role in achieving a more homogeneous and effective composite material, overcoming the challenges associated with filler incorporation into polymer matrices. The surface modification of filler materials can have varying effects on the piezoelectric properties of composites, depending on how it influences particle dispersion and interactions with the polymer matrix. For instance, Min et al. [26] demonstrated that the hydroxylation of PLZT (lead lanthanum zirconate titanate) particles can improve their dispersion and compatibility with a PVDF matrix. This resulted in a higher piezoelectric coefficient compared to composites containing untreated particles. In this case, the surface modification had a beneficial effect on the piezoelectric properties. On the other hand, Li et al. [27] provided evidence that the introduction of a coupling agent can have an opposing effect. They prepared PVDF/PZT composites by modifying the particles with silane and titanate coupling agents. They found that the silane coupling agent decreased the piezoelectric charge (d_{33}) and piezoelectric voltage (g_{33}) constants. This decrease was due to an insulating effect induced at the filler's surface. In contrast, the titanate coupling agent led to a maximum value of piezoelectric coefficients at specific content. So, in this case, the surface modification had a detrimental effect

on the piezoelectric properties. All the above highlights the importance of careful consideration when selecting and implementing surface modifications for filler materials in piezoelectric composites. The choice of modification and its impact on particle dispersion and interactions with the polymer matrix can significantly influence the resulting piezoelectric properties.

In this work, surface modification of NBT-BT particles was performed using two coupling agents, polar APTES and non-polar DDTES. The main objective is to find the best balance regarding the use of a special coupling agent and to examine its effect on the film structure, electrical properties, and potential for energy harvesting application. In the previous papers [11,12] we reported results on PVDF composites prepared without coupling agents. In this work, we investigated the effects of surface modification of NBT-BT particles in composites using two coupling agents, polar APTES and non-polar DDTES. It should be mentioned that although the use of coupling agents has been previously investigated for various materials [26-27], their effects on the final properties of the composites are still unclear. The main goal of this study was to find the best balance in terms of particular coupling agent utilization and to examine its effect on the film`s structure, electrical properties, and potential for energy harvesting application.

2. Experimental procedure

2.1. Powders preparation

Powders of composition $0.94[(Bi_{0.5}Na_{0.5})TiO_3]$-$0.06BaTiO_3$ (NBT-BT) were synthesized by solid-state reaction. The stoichiometric amounts of $BaCO_3$ (99.0%, Merck), TiO_2 (99.9%, Degussa), Na_2CO_3 (99.5%, Merck), Bi_2O_3 (99.9%, Aldrich) were ball milled in ethanol for 48 h and calcined at 800 ^oC for 1 h. Pressed pellets were sintered at 1150 ^oC for 30 min, crushed and sieved (as already reported in the previous work [11-12]).

2.2. Surface modification of NBT-BT particles using coupling agents

Two different silane coupling agents, namely, (3-aminopropyl)triethoxysilane (APTES) and dodecyl triethoxysilane (DDTES), were used for surface modification of the NBT-BT particles. The procedure used [28] consisted of the ultrasonic treatment of the dispersion of particles and silane in CH_2Cl_2 using a minimum volume of the latter (20 mL for 8.0 g of ceramic powder), but sufficient to allow silane absorption onto the particle surface; after the evaporation

of CH_2Cl_2, silane grafting on the particle surface was induced by heat treatment at 110°C for 1 h. To eliminate unreacted and/or ungrafted silane, the particles were rinsed twice with acetone.

The preliminary test, carried out to verify the effectiveness of the functionalization, revealed that the grafting yield for APTES was higher than that obtained by using DDTES, as shown in Table 1. Besides, by increasing the amount of APTES in the feed, the grafted amount of it increases. For DDTES, the TG characterization indicated that the surface modification is little dependent on the silane feed amount, with grafted amounts from 0.04 to 0.18 wt.%.

2.3. Preparation of polymer flexible films

Polymer films were fabricated by incorporating 30 vol% NBT-BT powders that had been modified using APTES and DDTES coupling agents into a commercial PVDF powder (Alfa Aesar) through a hot pressing method. For the comparison, a composite with the same composition but containing unmodified NBT-BT powder was also prepared. As-purchased PVDF polymer mainly has the non-polar α-phase of PVDF, but during the hot pressing, the generation of the electro-active β-phase can be induced in the neat polymer film (as previously published [11]). The complete hot pressing procedure can be found in the earlier papers [11,12]. Samples were named based on the active phase powder, as follows: NBT-BT/PVDF, NBT-BT-APTES/PVDF, and NBT-BT-DDTES/PVDF.

2.4. Characterization of modified powders and films

X-ray diffraction analysis of NBT-BT powder was conducted on a Bruker D8 Advance X-ray Diffractometer, while a Rigaku MiniFlex 600 diffractometer was used for the flexible films. The microstructure of films was investigated by a Tescan VEGA TS 5130MM instrument by observing the free surface and the cross-section of the composite films.

Infrared spectroscopy measurements on both, the powders and the composite materials, were taken in attenuated total reflectance (ATR) mode using a PerkinElmer Spectrum Two™ FTIR spectrometer. Spectra were collected in the wavelength range from 4000-400 cm^{-1}.

Thermogravimetric analysis (TGA) was carried out with a PerkinElmer TGA8000 analyzer. This technique was used to characterize the pristine ceramic particles and to estimate the amount of coupling agent grafted onto their surface as a consequence of the functionalization. After 5 min at 50°C the samples were heated from 50 to 700 °C at 20 °C/min

in N_2 atmosphere, then O_2 was introduced into the furnace and heating was continued up to 850 °C.

The crystallinity degree (X_C) of flexible films was quantified from the measurements performed at STA 6000 Perkin Elmer simultaneous thermal analyzer (TG/DSC). Heating from room temperature up to 200°C at a scan rate of 10°C/min under Ar atmosphere was performed. The percentage of crystallinity was obtained using the following equation 1:

$$X_c = \Delta H_m / \phi(\Delta H_{m100}) \text{ x } 100 \quad (1)$$

where H_m is the melting enthalpy of the PVDF composite films, H_{m100}=104.7 J/g is the enthalpy of the 100 % crystalline PVDF polymer, and ϕ is the fraction of PVDF in the composite (which is the same for all flexible films in this study) [11].

Dielectric measurements were conducted with an HP4284A LCR meter, covering a temperature range from 150 to 410 K and a frequency range of 100 Hz to 1 MHz, by using a four-wire probe. For temperature control during the measurements, the samples were positioned within a modified Linkam HFS600E-PB4 system.

Ferroelectric characterization was performed at Precision Multiferroic Test System with High Voltage Interface-Radiant Technologies, Inc. up to 4000 V at room temperature.

Anelastic measurements were conducted in the temperature range from 130 to 400 K. The measurement of the complex dynamic Young`s modulus $E=E` + iE``$ with the free flexural resonance method on rectangular strips suspended on thin thermocouple wires in vacuum was done. The Young's modulus was deduced from the resonance frequency f of the first flexural mode

$$E = \rho\left(\frac{fl^2}{1.028t}\right)^2 \quad (2)$$

where ρ, l and t are the sample's density, length and thickness. Since E varied of nearly two orders of magnitude between high and low temperature, the measuring frequency correspondingly changed of nearly 10 times. The elastic energy loss coefficient $Q^{-1} = E''/E'$ was measured from the width of resonance peak.

Piezoelectric measurements were performed by employing an apparatus which applies an electrical signal at 2 MHz to a transducer which converts it into an acoustical signal. The acoustical signal is applied to the composite film which converts it through piezoelectric effect into an electrical signal, which is measured by an oscilloscope. The piezoelectric charge constant (d_{33}) values have been obtained from comparison with the reference piezoelectric signal

measured on a $LiNbO_3$ single crystal plate in the same configuration setup. The piezoelectric voltage (g_{33}) constant values have been obtained by using the well-known formula $g_{33}= d_{33}/\varepsilon_{33}$.

2.5. Poling, film assembly and testing

The samples were electrical polarized in a silicon oil bath (as described in the previous publications [11,12]). In order to isolate and protect the flexible films (4 cm^2) from surroundings, after poling and wiring, they were integrated into a flexible Kapton layer (polyimide film).

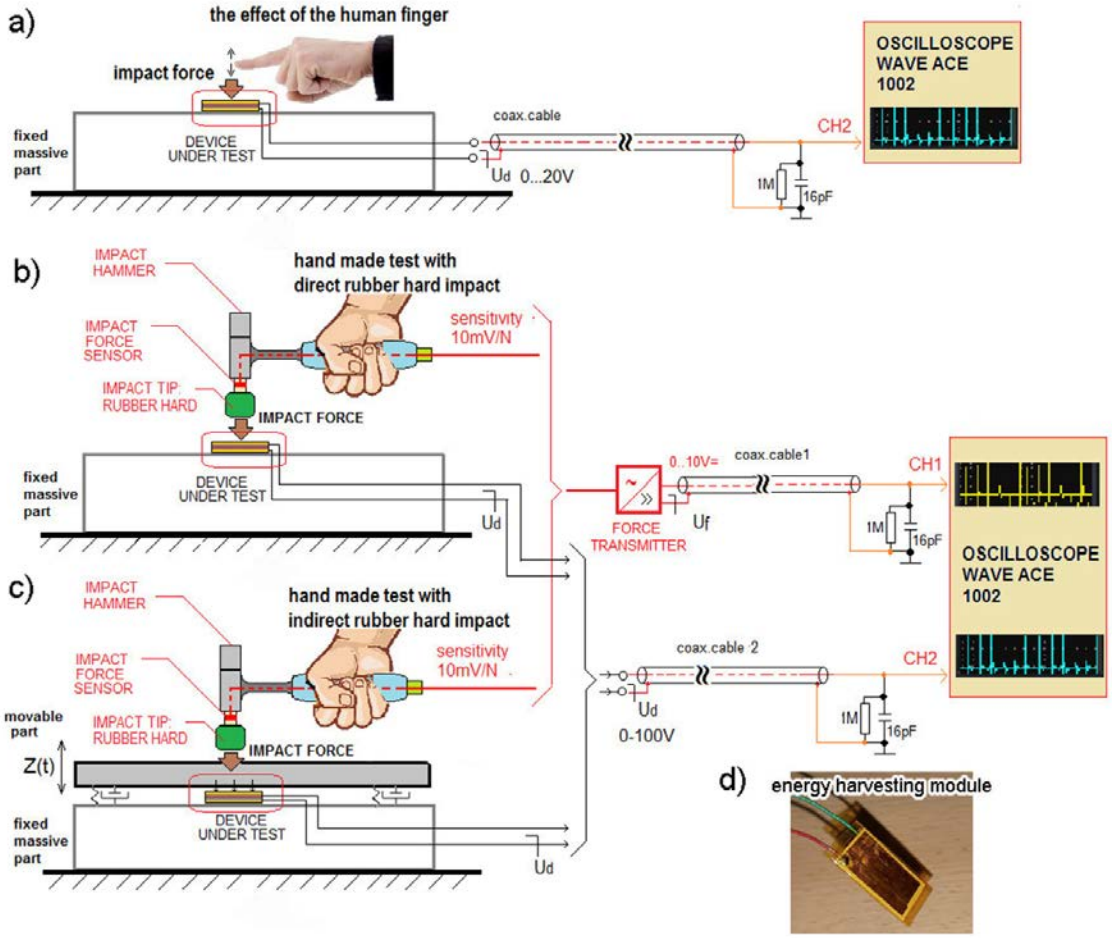

Figure 1.a-c) Schemes of energy harvesting testing set-ups and d) energy harvesting module

The energy harvesting efficiency tests were performed using a custom-made laboratory apparatus. Schemes of the setups for testing are presented in Figure 1a-c. The energy harvesting

potential was measured by three different tests under force impact. Firstly, the experimental test by tapping with the index finger (FT-finger tapping) was performed. Then, to get more uniform distribution of mechanical stress on the sample, the mechanical impact was produced by a hammer (Quartz Impulse hammer with Integrated Electronics Piezo Electric output modal, KISTLER, Italy) with a rubber end of 2 cm in diameter. Finally, the sample was placed in the holder between sandwich-like metal plates with two springs at the ends of the bottom plate to get even more uniform pressure on the investigated samples. After each mechanical impact of the impulse hammer, springs return the upper metal plate to the initial position (see scheme in Figure 1c).

3. Results and discussion

3.1. Characterization of powders

The phase composition of unmodified NBT-BT powder, produced following the procedure reported in 2.1, was assessed by XRD analysis. The registered XRD (Figure 2a) shows that the pure perovskite NBT-BT phase is obtained (JCPDS 63-0299) without any secondary phases. Moreover the evidence of the splitting of the peaks at ~ 40 and 46.5 ^{o} (inset graphs of Figure 2a) confirms the coexistence of the tetragonal and rhombohedral phases [29] typically observed at the morphotropic phase boundary (MPB), at which solid-solution piezoelectric materials attain the maximum of their functional properties.

The functionalization of the NBT-BT powders by APTES and DDTES was investigated by ATR-FTIR analysis (Figure 2b). The three spectra of unmodified and silane-modified powders exhibited a strong absorption band about 530 cm^{-1} which is assigned to the Ti-O stretching mode characteristic for $BaTiO_3$. In the spectra of modified powders, Si-O-Si and Si-O-C stretching vibrations can be noticed in the range 1000-1200 cm^{-1} which confirms the presence of silane moieties at the surface of the NBT-BT particles (left inset in the Figure 2b). Two more small bands are visible around 1400-1500 cm^{-1} and can be related to asymmetric vibration bands of CH_3 and in-plane deformation of CH_2. Furthermore another absorption around 1570 cm^{-1} can be attributed to the amino group bending of APTES modifier. Small bands at 2850 and 2960 cm^{-1} showed asymmetric and symmetric CH_2 stretching vibrations of the alkyl chains of both APTES and for DDTES (the right inset in Figure 2b) [11].

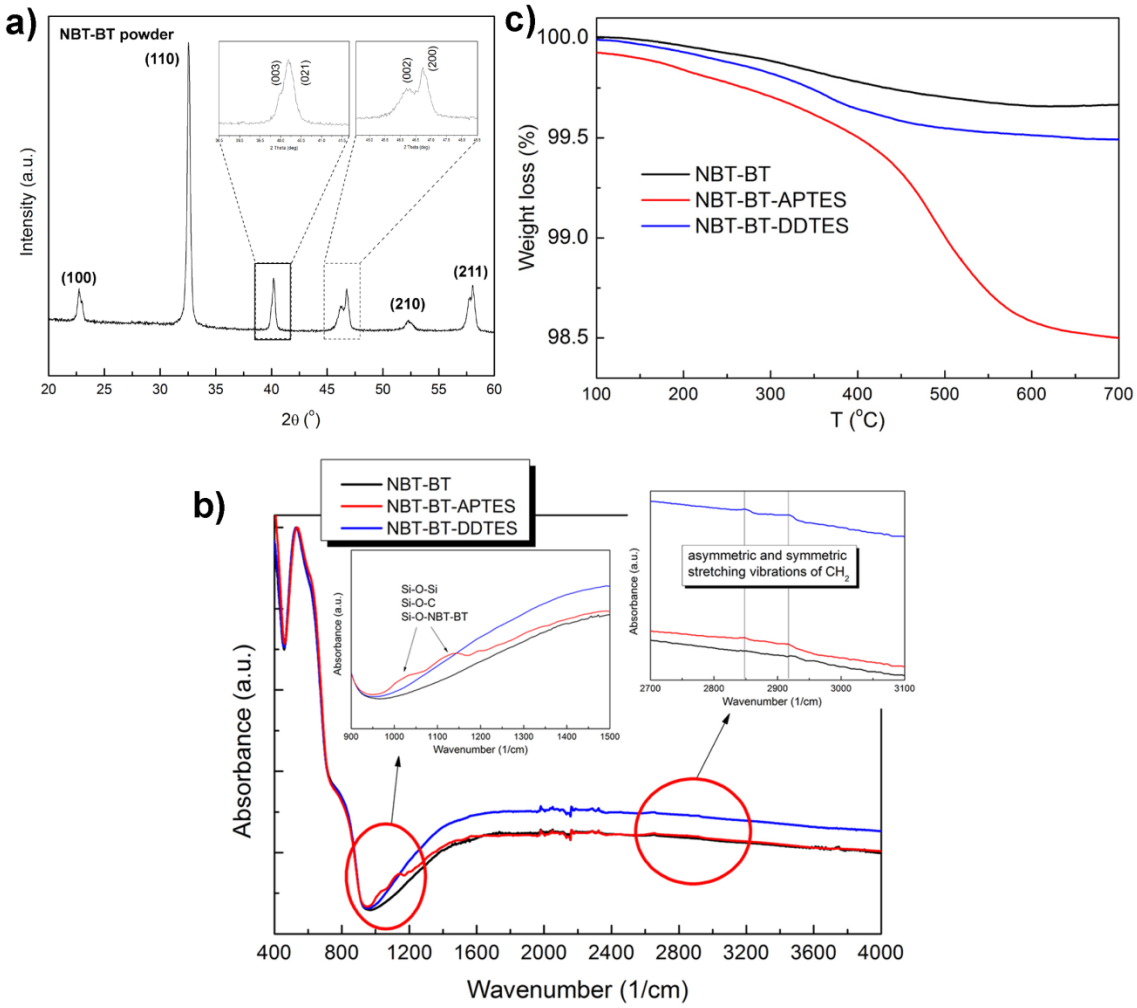

Figure 2. a) XRD pattern of NBT-BT powder, the insets report the magnification of the pattern in the 38-41 and 44-48 ° 2θ range, b) Infrared spectra of non-modified and surface modified NBT-BT powders, c) TG curves for non-modified and silane-modified NBT-BT powders, shown in the temperature range 100-700 °C

TG thermograms of all powders, presented in Figure 2c, showed, as expected, some differences between unmodified NBT-BT and powders modified with the coupling agents. Weight loss during the heating from 50 up to 700 °C was 0.33 % for pure NBT-BT powder to 0.5 and 1.2 % for powders modified with DDTES and APTES, respectively. Subtracting the weight loss of the unmodified powder, the grafting degrees resulted 0.86 and 0.15 wt% for APTES and DDTES, respectively (see Table 1).

Table 1. NBT-BT particles surface-modified with silane coupling agents, corresponding fed and grafted amounts

Sample	Silane	Feed (wt.%)	Grafted (wt.%)
NBT-BT-APTES	APTES	**2.5**	**0.86**
NBT-BT-DDTES	DDTES	**15.0**	**0.15**

Examination of the thermograms, evidenced that up to 150-200 ^{o}C the weight loss is associated mainly with physically adsorbed water. For the unmodified NBT-BT powder a slight weight loss occurs along the whole temperature span, due to condensation of surface hydroxyl groups. A second weight loss, starting from below 400 °C and with DTG peak (maximum of the degradation rate) just above 500 °C, was recorded for the modified powders. It can be connected with the thermal decomposition of the organic moieties of APTES and DDTES grafted to the powders, which is superimposed with the condensation of Ti-OH and Si-OH remaining on the surface.

3.2. Characterization of flexible films

3.2.1. Structural characterization

The microstructures of free and fracture surfaces (as insets) are presented in Figure 3. The free surface of the films shows the homogeneous distribution of the active phase in the PVDF matrix. A closer look at the fracture surface indicates the formation of active phase agglomerates in all three types of films. The highest agglomeration degree was noticed in the films modified with the DDTES coupling agent.

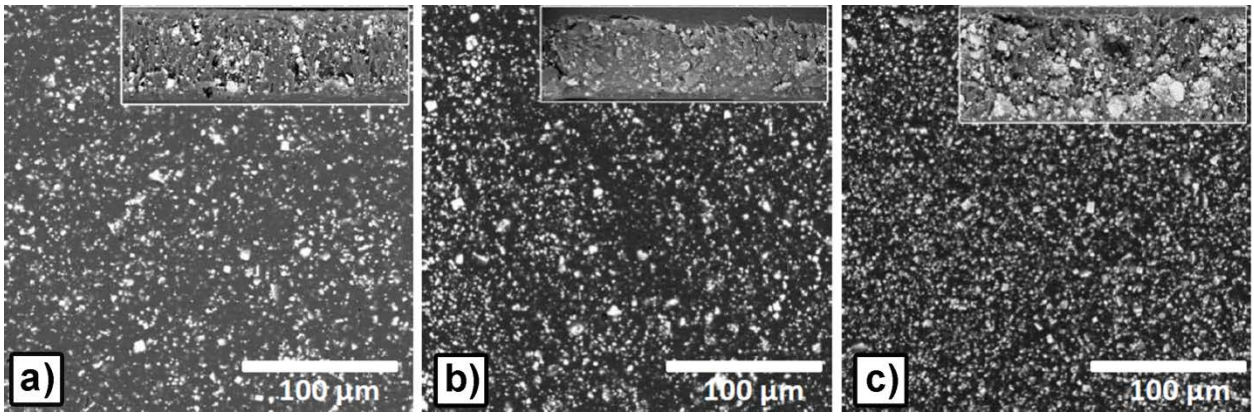

Figure 3. SEM micrographs of flexible films obtained from a) non-modified NBT-BT powders, b) NBT-BT modified with APTES and c) NBT-BT modified with DDTES

During previous investigations [11], high temperature and pressure during the hot pressing procedure resulted in the change of α-PVDF into electrically active β and γ-phases. Besides the hot pressing conditions, the presence of ceramic fillers and, here, of an organic modifier (i.e. APTES and DDTES) strongly affected the crystalline structure of the polymer matrix by changing its polymorphism (α, β and γ-phases). XRD results of all composite films evidenced the simultaneous existence of different PVDF polymorphs (Figure 4a).

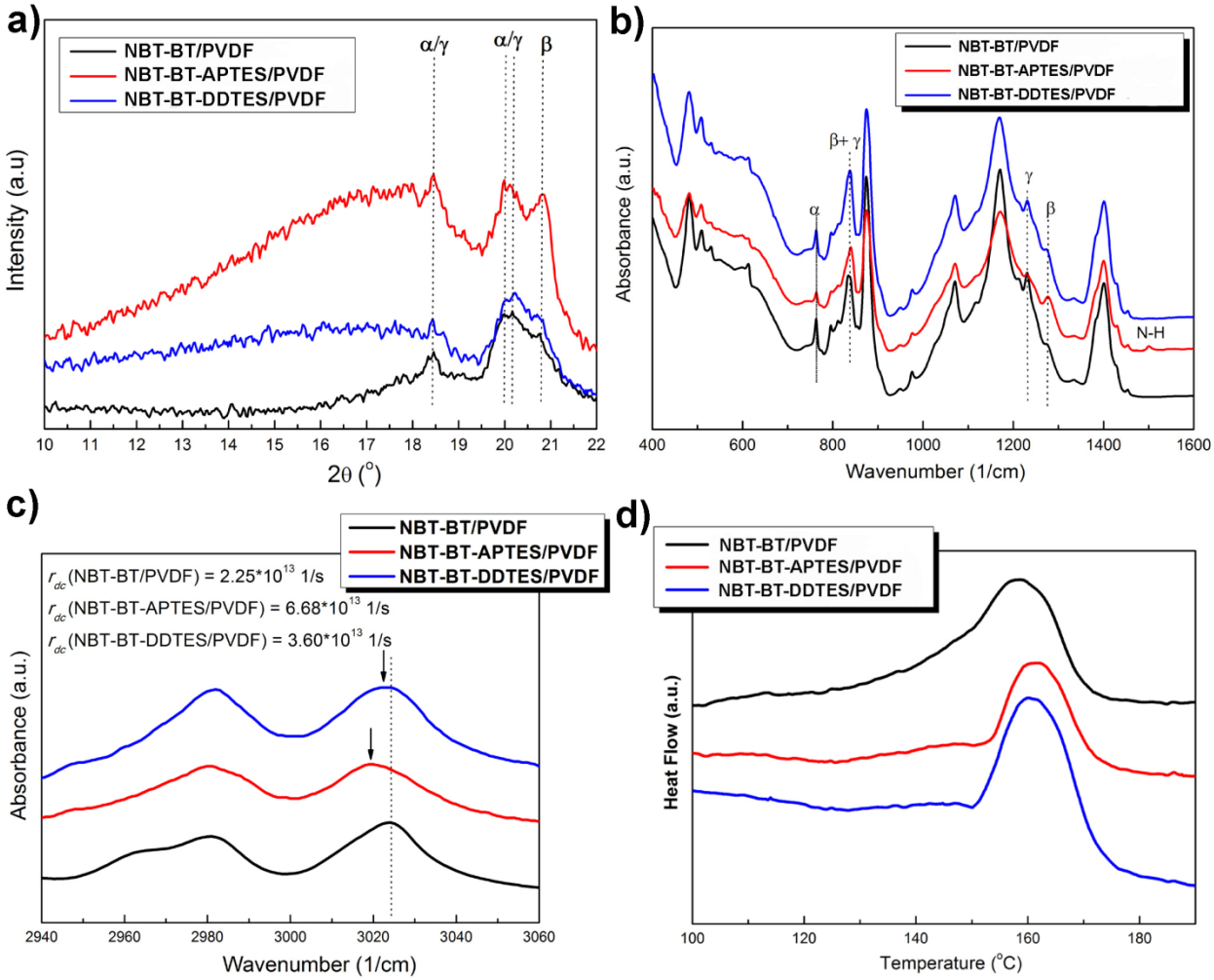

Figure 4. a) XRD pattern for modified and non-modified composite films, b) Infrared spectra of the PVDF-based films consisted of NBT-BT powders without surface modification and surface modified powders with APTES and DDTES coupling agents, before poling procedure, c) region 2940-3060 cm^{-1} with calculated damping coefficients, d) DSC thermograms of hot pressed composite flexible films made of non-modified NBT-BT and samples modified with APTES and DDTES coupling agents

Diffraction peaks at 17.7, 18.4, and 20.0 ^{o} coincide to (100), (020), and (110) reflections of the monoclinic α- phase crystals (JCPDS #042-1650), respectively. A peak at 20.8^{o} that is

related to the sum of the diffractions at (110) + (200) planes of the orthorhombic β-phase (JCPDS #042-1649), proves the existence of this polymorph in all flexible films, and it is especially evident for the APTES-modified sample. Diffraction peaks, characteristic of γ-phase, can be expected at 18.5, 19.2, and 20.0^{o}, that is at 2θ values very close to the reflexions that belong to the other two polymorphs [11, 30]. It is also worth noting that the amorphous halo in the region 14-18^{o}, visible for both silane-modified composites, is mostly evident for APTES-modified samples.

FTIR spectra of all flexible films were recorded and analyzed to obtain a more detailed analysis of formed PVDF polymorphs in each flexible film. The relative fraction of the electro-active phase(s) (F_{EA}) on normalized spectra was obtained using the equation that can be found elsewhere [31-33]:

$$F_{EA} = \frac{I_{EA}}{1.26\, I_{\alpha} + I_{EA}} * 100 \qquad (3)$$

where I_{EA} is the absorbance of the band at about 840 cm^{-1} that can be assigned to β and/or γ phase, I_{α} the absorbance of a characteristic band of the α phase at 763 cm^{-1}, and 1.26 the ratio between the absorption coefficients at the respective wavenumbers. According to X. Cai *et al.* [34], when β and γ phases exist side by side, the peak-to-valley height ratio between the two peaks around 1275 (β-phase) and 1234 (γ-phase) cm^{-1} is used to separate their two contributions (F_{β} and F_{γ}). The FTIR results of flexible films filled with the three different NBT-BT powders, are presented in Figure 4b. Details about all characteristic bands used for the identification and quantification of all PVDF polymorphs present in the FTIR spectra can be found in a previous study [11]. Summarizing, all characteristic peaks for α-, β- and γ- PVDF polymorphs are present in all prepared flexible films (marked in diagrams).

Nevertheless, using equation 3, values for different PVDF polymorphs in all the investigated samples are extracted and presented in Table 2. The highest percentage, 67% of total electroactive PVDF polymorphs was obtained in both modified samples. In the NBT-BT-DDTES sample, predominantly γ-phase was formed, since the peak on the FTIR spectrum, which shows the contribution of β phase (1275 cm^{-1}) is shoulder-like, and its quantification is rather difficult for these samples. On the other hand, in the sample modified by APTES, out of 67% of electroactive phases, 52% was β- phase, according to the results obtained from the XRD analysis.

Table 2. Calculated amounts of PVDF polymorphs extracted from FTIR measurements (before polarization procedure) with overall crystallinity degree quantified from DSC analysis

SAMPLE	α (%)	β (%)	γ (%)	F_{EA} (%)	X_c (%)
NBT-BT-APTES/PVDF	**33**	**52**	**15**	**67**	**38**
NBT-BT-DDTES/PVDF	**33**	**5**	**62**	**67**	**50**
NBT-BT/PVDF	**45**	**4**	**51**	**55**	**53**

Chandran et al. [22] noticed the same in their multiwall carbon nanotubes-PVDF composites. They performed the functionalization of nanotubes by APTES and after the preparation of composites with PVDF by solvent casting method, they predominantly noticed the formation of β- phase. In another study, A. Chandran et al. [35] showed that the PVDF composites prepared using surface functionalized ZnO nanoparticles improved the creation of the polar β- phase in these polymer composites as well. The enhanced formation of β- phase in APTES samples can be explained by more pronounced interaction of APTES coupling agent with PVDF chains. In these samples the formation of hydrogen bonds between 1) the F atoms of the polymer chain and the H atoms of the amino group of the silane and/or 2) between H atoms from the PVDF chain and N atoms from the coupling agent are possible [36]. While, in the DDTES-modified samples only bonds between the H atom and C can be formed (Schematic presentation is given in Figure 1.). The mechanisms of possible interactions between modified particles and PVDF are schematically represented in Figure 5.

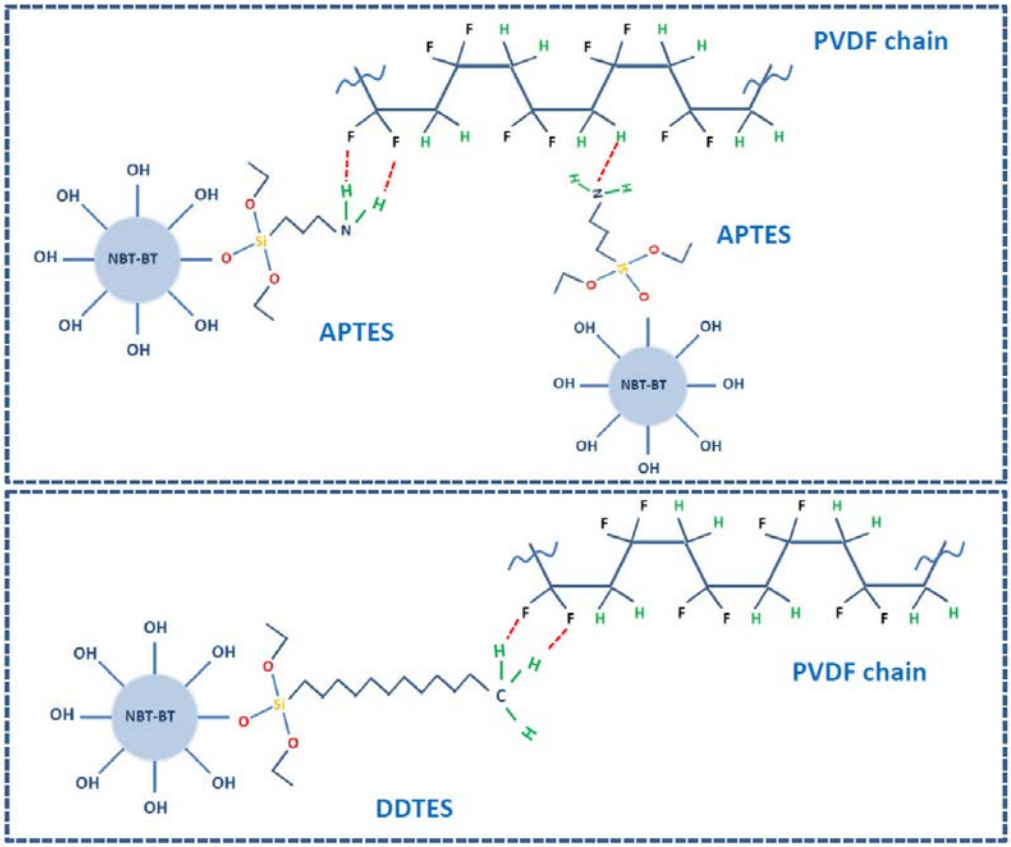

Figure 5. Scheme of silanization of NBT-BT particles using APTES and DDTES coupling agents and connection of functionalized particle with PVDF chain (the connection is depicted only for one bond with particle)

It is important to add that in the non-modified samples, 55% of γ-phase coexists with non-polar α-phase which is very close to the result obtained for neat PVDF film [11].

Additional explanation can be given through the analysis of the 2940-3060 cm^{-1} region which is assigned to the asymmetric and symmetric -CH_2 stretching vibrations related to the interfacial interactions between the particles of the filler and polymer chains. In the modified samples, the band near 3025 cm^{-1} has shifted toward the lower wavenumber region, compared with the non-modified one (Figure 4c). The interfacial interaction between -CH_2 dipole and filler particles lowers the vibrational energy and causes the damping effect. Thus, it was suggested that this variation in the peak's positions can be explained with the damped harmonic oscillation model [35]. The effect of the electrostatic interaction between the filler particles and -CH_2 dipole can be determined through the calculation of the damping coefficient, r_{dc} from the equation 4:

$$r_{dc} = 4\pi c \left(\nu_{polymer}^{2} - \nu_{composite}^{2}\right)^{0.5} \qquad (4)$$

where c is the velocity of light and ν is the wavenumber of -CH_2 damping free vibration. The damping coefficient values obtained for modified samples were higher in comparison with non-modified sample (values given in Figure 4c). The highest value of this coefficient was calculated for APTES modified films, suggesting enhanced electrostatic interaction of filler particles, that possess amine groups, with PVDF chains. Consequently, the highest percentage of polar β-phase was formed particularly in APTES-modified films [35].

At this point, DSC measurements were significant to investigate melting point (T_m) and percentage of crystallinity (X_c) of the prepared composite films. As can be seen from Figure 4d, the DSC curves do not show multiple melting peaks or shoulders that can point to the formation of different polymorphs. There is only one broad endothermic peak in the 140-170 ^oC temperature range that corresponds to crystal melting, possibly suggesting the overlapping of characteristic melting regions. The melting point (T_m) of composite made of non-modified NBT-BT is quite broad and mostly centred at 158 ^oC. In the silanized samples a substantial change in the position of the melting peak can be observed, that moves toward higher temperature at ~ 162 ^oC. According to the literature, the PVDF melting behaviour depends on polymorphism on one side and characteristics such as crystallite size, defects, inclusions, etc. on other side [31]. In their review of neat PVDF, P. Martins et al. explained that there is an evident difference in melting points of various PVDF polymorphs. The melting peaks of α- and β- phases are in the 160-172 ^oC temperature range, while the γ- phase shows the endothermic peak at higher temperatures, ~180-190 ^oC. It should be also emphasized that the procedure used for the preparation of PVDF films has a high impact on the melting peaks position as well [37]. For instance, when the γ-phase is obtained by crystallization from the melt, the melting temperature is about 10 ^oC lower than the melting temperature of PVDF film obtained from direct α- → γ- phase transformation (180-190 ^oC) [33,37-38].

As a result, here, the exact conclusions regarding the formation of particular PVDF phases cannot be given from DSC analysis. The DSC method can be only taken as a complementary technique to FTIR analysis since the PVDF films melting behaviour can be affected by the preparation procedure, and many crystalline defects can emerge in the films by the addition of non-modified and modified NBT-BT particles.

Even in pure PVDF, due to structural defects, crystallinity is commonly limited to 50-60 % [35, 39-41]. As evident from the results, the addition of filler particles did not greatly reduce

the PVDF total crystallinity degree. The unmodified and DDTES-modified samples were found to possess a crystallinity of ~ 50% while the APTES-modified ones have a lower value of crystallinity value, ~ 38% (Table 2).

3.2.2. Electrical properties of flexible films

3.2.2.1. Dielectric properties

The temperature dependence of dielectric permittivity and dielectric loss tangent measured at various frequencies on the flexible films (obtained from powders modified with APTES and DDTES and non-modified NBT-BT powders) is presented in Figure 6. The values of dielectric permittivity obtained for silane-modified samples are a bit lower in comparison with pure NBT-BT/PVDF films in the whole temperature range. Although ε` for all three films is lower than for NBT-BT ceramics (~ 2000), it is higher than ε` of pure PVDF film (~10) [11].

As expected, the addition of active phase particles in the PVDF matrix enhanced the dielectric permittivity of the polymer composite films. According to different papers that dealt with PVDF composite films, the dielectric permittivity and losses are highly related to the active phase amount, microstructure, and agglomeration, as well as to the properties of the polymer matrix [42-43]. Due to the high amount of polymer in the films (70 vol%), there are large areas of the polymer matrix that affect the overall permittivity of the composite. From Figures 6a-c) one can state that the general trend in dielectric properties diagrams is pretty much similar for all investigated flexible films. The dielectric properties, in the investigated temperature range, are primarily governed by the effects of interfacial and dipolar polarization. At temperatures below 200 K dielectric permittivity and losses are temperature-independent due to the existence of frozen dipoles (primarily C-F dipoles of polymer). In the 210-325 K temperature region, for 0.2-200 kHz frequencies the increase of both ε` and tan δ was noticed due to the well known α_a-relaxation, which is associated with the glass transition of the PVDF polymer. When the glass transition temperature is reached, chain segments in amorphous regions start to move, resulting in local micro-Brownian motion of molecular segments. Consequently, the ε` values increase and tan δ forms a consistent peak [40]. The third notable region, above 325 K, in which dielectric permittivity and loss tangent increase again, can be attributed to the mobility of the crystalline part of the polymer chains, known as α_c -relaxation. The peak associated with this relaxation is out of the experimental window and/or is covered by conduction effects. According to the

literature data, there are a couple of possible sources of interfacial polarization that mostly can affect dielectric relaxations: (1) polarization due to the accumulation of space charge in the interface region between PVDF matrix and filler particles and/or (2) polarization at the boundaries between the crystalline and amorphous PVDF phases [40,44,45,46]. Interfacial polarization in non-modified samples is higher than in modified samples. In the latter the filler particles are anchored to the PVDF matrix through the silane coupling agents, that lowers the interfacial tension between particles and polymer. Consequently, the modified samples have lower dielectric permittivity values.

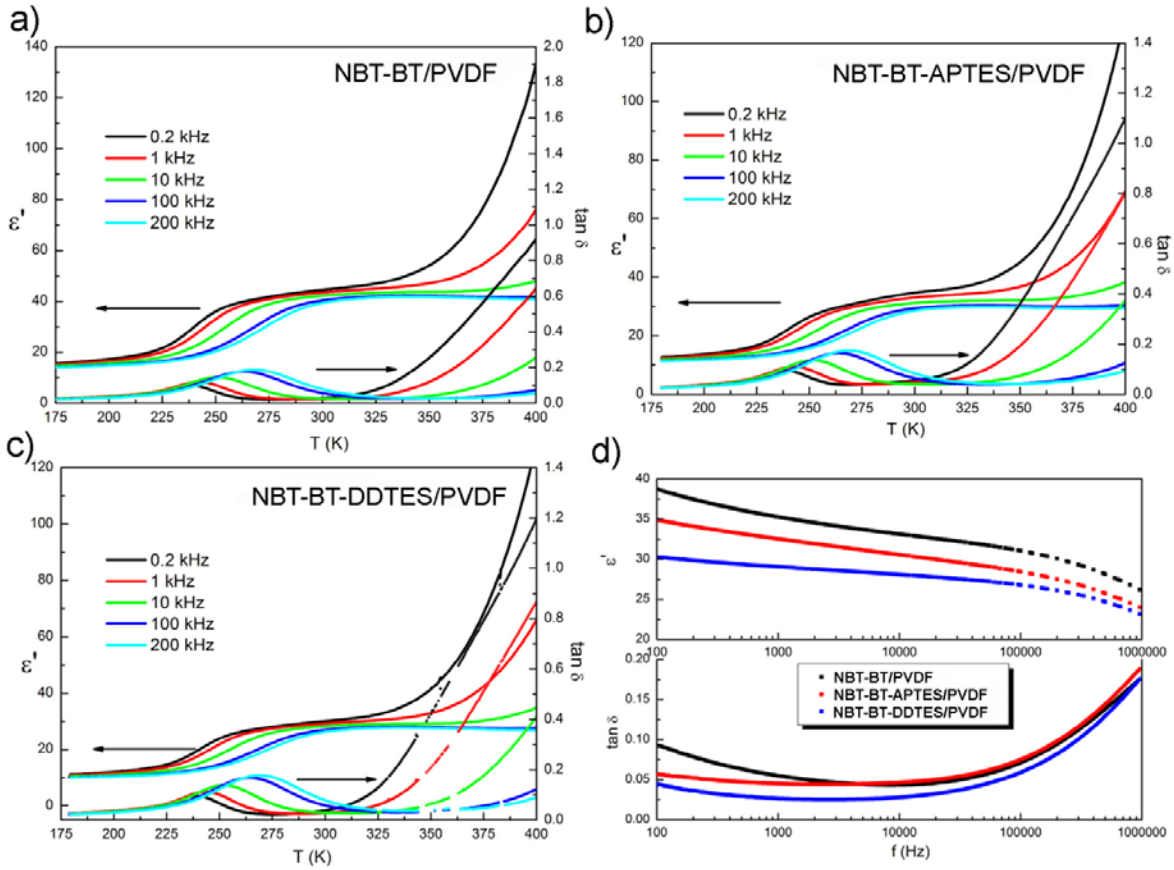

Figure 6. Dielectric permittivity and loss tangent vs. temperature for a) NBT-BT/PVDF, b) NBT-BT-APTES/PVDF, c) NBT-BT-DDTES/PVDF and d) dielectric permittivity and loss tangent vs. frequency for all investigated samples at room temperature

Additionally, the type of PVDF polymorph formed in the flexible film is considered an important factor that can influence the dielectric properties, especially dielectric losses, of the films [36,40,47,48]. A high dipole arrangement is expected in the films in which polar PVDF phases were formed. In the samples modified by APTES, more polar β-phase was formed while

in DDTES ones mostly γ- phase exists (which is also polar, but with a lower dipole moment than β-phase). The increase of β-phase amount in the APTES samples affects the increase of the net dipole moment in the unit cell, which contributes to dipolar polarization and the higher dielectric permittivity of these modified samples [35,40,42,44]. Rui et al. studied the influence of dipole mobility on dielectric properties in the PVDF [49-50]. They concluded that dipoles found in the amorphous part of the PVDF matrix are larger and highly mobile. This can also lead to a dielectric permittivity increase. Since a higher amount of amorphous phase was found in the samples modified with APTES, in comparison with those modified with DDTES, this explains the higher values of dielectric permittivity and losses obtained for these samples.

The dependence of dielectric permittivity and loss tangent on frequency, in the 100 Hz-1 MHz frequency range at room temperature, is presented in Figure 6d. In general, regarding dielectric losses, high values of tan δ in the low-frequency region are attributed to the interface relaxation polarization losses, while its increase in the high-frequency region is related to the dipolar relaxation [45]. More precisely, losses are affected by the Maxwell-Wagner-Sillars mechanism in the low-frequency region [40,46], that has its origin in interfacial polarization and appears in partially crystalline or semicrystalline materials, like the investigated ones. Therefore, higher values of tan δ, in this frequency region, were registered for non-modified samples due to the existence of more developed interfaces between the incorporated NBT-BT particles and PVDF matrix.

As explained above, coupling agents reduce the interfacial tension between particles and polymer and limit the accumulation of space charges at the interfaces, so the dielectric losses are lower than in non-modified samples. However, in the high-frequency region, the dielectric losses of APTES-modified samples are higher, indicating the effect of the previously mentioned dipole polarization relaxation [49-50].

3.2.2.2. Mechanical properties

Figure 7 shows the Young's moduli E and elastic energy loss coefficients Q^{-1} of the three studied materials, measured during cooling at <1 K/min exciting the first flexural modes. The resonance frequencies were f = 200-400 Hz at room temperature, but varied of a factor up to 10 between the minimum and maximum temperature, since $f \propto E^{1/2}$. It appears that the temperature dependences of both the Young`s moduli and the acoustic losses are dominated by those of the

polymer, with the α_c relaxation around 320 K and α_a relaxation at 240 K, visible also in the dielectric spectra.

The Young's modulus of ceramic NBT-BT rises almost linearly from ~100 GPa at 400 K to ~140 GPa at 100 K, being 40 times larger than that of PVDF at room temperature, and therefore the ceramic inclusions only increase the magnitude of the elastic modulus of the composite (Table 3). If we assume that the differences in rigidity between the three samples are due to differences in cohesion between the ceramic particles and the PVDF matrix, it results that NBT-BT/PVDF, with untreated ceramic particles, has the smallest cohesion, as expected, while the DDTES treatment is the most efficient in promoting the mechanical cohesion. The degree of crystallinity of the polymer and its elastic properties seem to play a secondary role in determining the effective modulus of the composite.

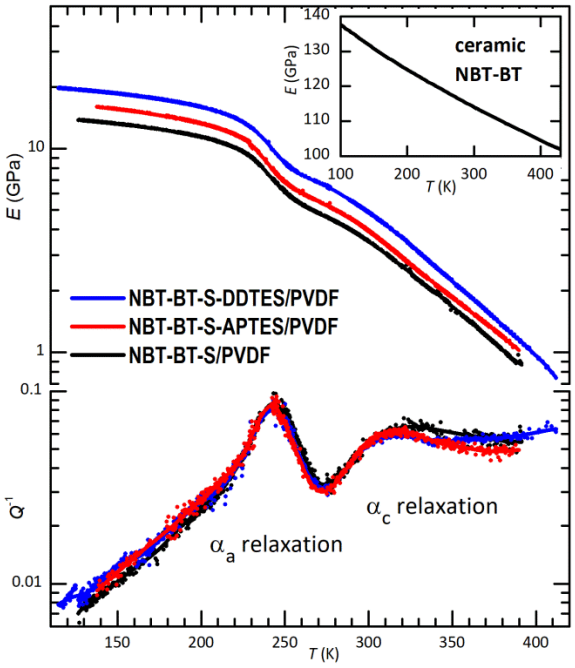

Figure 7. Young's modulus *E* and elastic energy loss coefficient Q^{-1} of the three studied materials, measured during cooling at <1 K/min

Table 3. Density, Young`s modulus, mechanical losses, dielectric permittivity and dielectric losses of all investigated flexible films at 295 K

SAMPLE	ρ (g/cm^3)	*E* (GPa)	tan δ_m	ε'	tan δ_e
NBT-BT-APTES/PVDF	**2.929**	**4.22**	**0.048**	**32.5**	**0.045**
NBT-BT-DDTES/PVDF	**2.985**	**5.18**	**0.048**	**29.04**	**0.026**
NBT-BT/PVDF	**2.989**	**3.73**	**0.048**	**35.3**	**0.055**

3.2.2.3. Ferroelectric properties

Ferroelectric hysteresis loops for all examined samples measured at the breakdown field are presented in Figure 8. The loops are well defined but not saturated, therefore the parameters such as remnant polarization, coercive filed, etc. cannot be extracted from the diagrams with high precision. To explain the ferroelectric properties of composites, firstly, the properties of the filler and PVDF matrix separately should be considered. In the previous study, well-saturated square shaped hysteresis loop for NBT-BT ceramics (with P_r = 38 μC/cm^2 and E_c = 30 kV/cm measured at 50 kV/cm) and linear-shaped ferroelectric properties for pure PVDF film were obtained [11]. The composites hysteresis loops are apparently under the profound influence of NBT-BT particles in the films since P_r increases by increasing the applied electric field. The loops of the modified samples show pretty similar shapes but it is obvious that the sample modified with the APTES coupling agent was able to withstand higher applied fields than the one coupled with DDTES. The non-modified sample was able to reach 150 kV/cm but with the formation of a very lossy hysteresis loop. According to the literature, there are many possible reasons, from already mentioned interface areas of different kinds and crystallinity (explained in the dielectric properties section) up to microstructure, agglomeration of the filler, and the formation of voids in the polymer matrix [9,11,12,14,19].

It is well known that neat PVDF films can contain predominantly α-, β- and/or γ- phases and each phase possesses different ferroelectric properties [11,42,51,52,53]. Therefore, the effect of the formed PVDF polymorphs and their crystallinity degree in the composite films should be first considered. Having in mind that β- and γ- phases are polar PVDF polymorphs, among which β- phase is considered as the most polar one and with typical characteristics of ferroelectrics, samples with the highest amount of this phase are the ones modified with APTES. These samples consequently have shown the best ferroelectric properties. Non-modified and DDTES-modified samples have mainly γ- phase, that is also polar, but slightly lower properties were obtained.

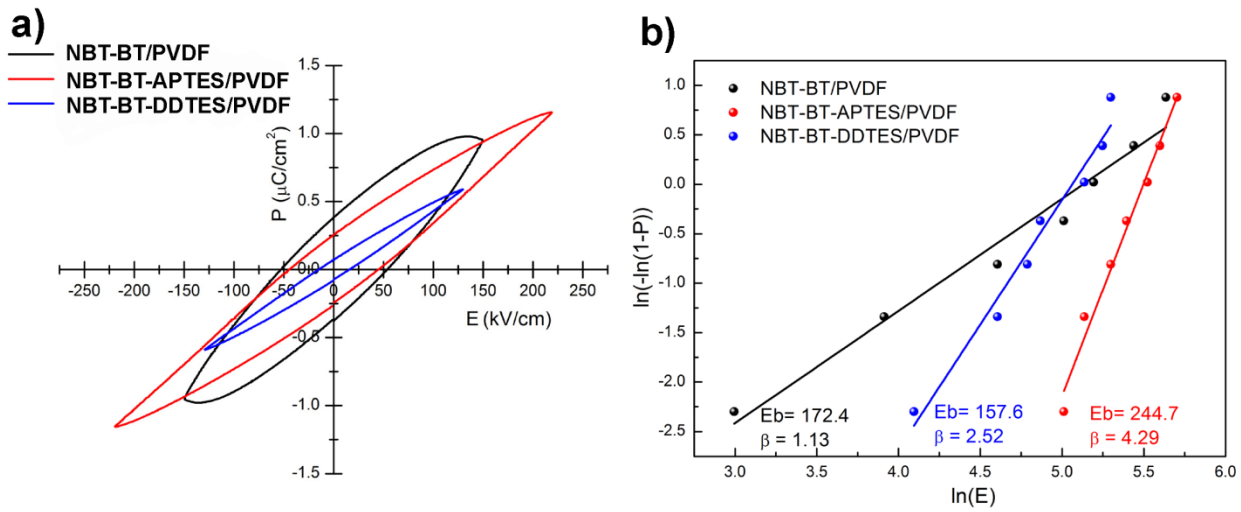

Figure 8. a) P-E hysteresis loops for non modified NBT-BT/PVDF films and silane APTES and DDTES modified NBT-BT/PVDF films at room temperature and break down field for each sample, b) Weibull distribution of the breakdown strength

Additionally, some authors studied different types of amorphous fractions and, accordingly, dipole motions that can influence the ferroelectric properties of the PVDF films [54]. As reported by them, in the amorphous part of the PVDF, from the chain mobility point of view, rigid and mobile fractions of the polymer chains are possible. A mobile fraction (MAF), also called isotropic amorphous part, and a rigid fraction (RAF), an intermediate fraction between the crystalline part and mobile amorphous part of the polymer, are schematically presented in Figure 9. Furthermore, the rigid part of the amorphous fraction quickly devitrifies above the glass transition temperature and becomes mobile at room temperature. Therefore, it can be speculated that the amorphous part of the APTES-modified samples possesses more mobile fractions which enable the formation of ferroelectric domains and enhance the ferroelectric properties of this film. However, much deeper study and analysis are necessary to explain these assumptions which can be a subject of future investigations.

P. Mao et al. in their study about PVDF-PTC composites suggested that a greater elastic modulus and excellent intermolecular interactions between polar groups in the polymer composite films may help the enhancement of its breakdown strength [45]. Accordingly, the modified films possess larger elastic modulus (Table 3) but only APTES-modified samples show higher breakdown strength. In non-modified samples the poor connectivity of NBT-BT particles to the polymer matrix is the controlling parameter for ferroelectric properties. These high dielectric constant NBT-BT inclusion particles generate local electric fields at the polymer

interface that are higher than the externally applied field. Assuming that the branching of conductive paths directly passes through the solid NBT-BT particles and leads to the reduction of the electric breakdown strength [55].

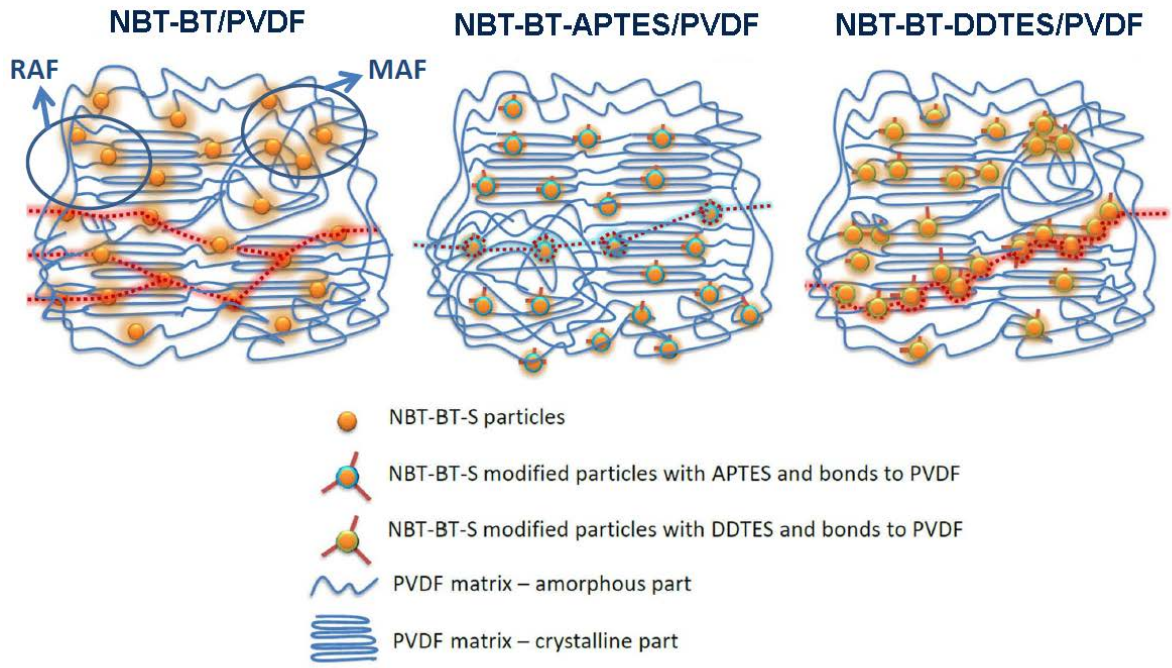

Figure 9. Schematic presentation of possible conduction paths in non modified and modified polymer composite

The addition of coupling agents is one of the possible approaches to smooth the inhomogeneous distribution of the electric field and to suppress the charge carrier movement [18]. It should be taken into account that not any coupling agent will give the desired properties and it must be carefully selected. Hence, NBT-BT particles modified with DDTES were prone to agglomeration and therefore the formation of "hot spots" in which the electric field among connected particles is much higher in comparison with the applied electric field (especially if they are aligned with the applied field) and leads to the faster electrical breakdown. Possibly, the DDTES layer can block the ramification of the conduction paths but structural defects clearly have a dominant effect. The direct contact of particles forms a pathway for conduction charges, leading to the deterioration of the breakdown strength [56,57,58]. Modification with APTES has led to a more homogeneous distribution of NBT-BT particles in the film. It can be assumed that the interface architecture formed in these samples, traps the space charges and limits the formation of

conduction channels through the sample, allowing higher breakdown strength. A schematic presentation of possible conduction paths that simulate the breakdown processes in each composite is presented in Figure 9.

Electric breakdown strength can be also analyzed by the two-parameter Weibull distribution through equation 5 [43, 45]:

$$P(\mathrm{E}) = 1 - \exp\left[-\left(\frac{E}{E_b}\right)^{\beta}\right] \qquad (5)$$

where P(E) is the cumulative probability of electric failure, E is the experimental breakdown strength, E_b is the characteristic breakdown strength at the cumulative failure probability of 63.2%, and β is the Weibull modulus associated with the linear regressive fit of the distribution. The Weibull plots of all investigated composites together with the values of Weibull breakdown strength, Eb, and Weibull modulus, β are presented in Figure 8b. The breakdown strength value is the highest for the APTES-modified sample, proving that stronger intermolecular interactions between APTES silanized filler particles and PVDF chains enable enhancement of the breakdown strength of these films [43,59]. The Weibull modulus is used to determine the quality and structural integrity of the films. According to the obtained data, β values are higher for both types of modified samples, indicating a positive effect of particle silanization on the structural quality of the films. A similar trend of conduction through the films and interface effects was also noticed by other authors that studied various ceramics functionalized by different silane coupling agents, dopamine, etc. in the PVDF matrix. They also pointed on the importance of interface tuning to get high-performance devices with high electrical breakdown strength [16,23,57].

3.2.2.4. Effect of poling on PVDF phase transformation

It is well known how important is the process of polarization of active phase implemented in the PVDF polymer composites [44,60-61]. Many studies were focused on exploring the methods of PVDF film polarization emphasizing its importance for further applications of polymer composite harvesters [30,62,63].

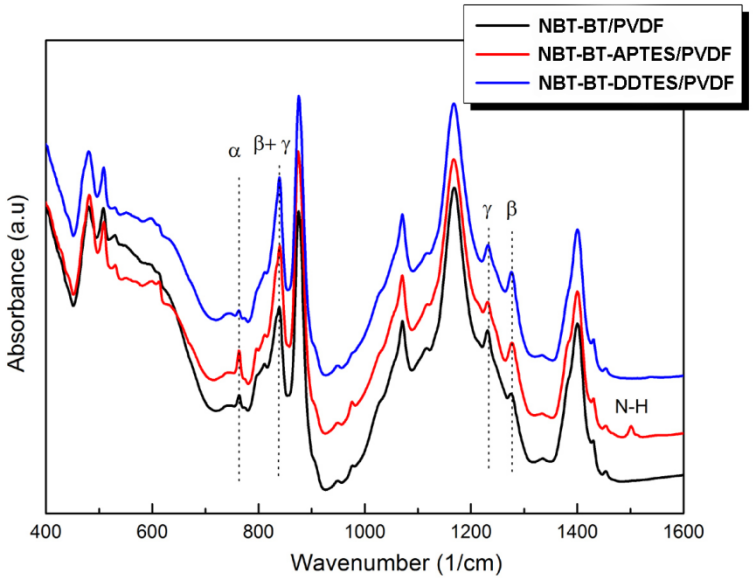

Figure 10. Infrared spectra for all flexible films, after polarization procedure

Poling induces differences in the crystalline organization: in the poled materials there is a more oriented structure where the dipole moments are directed towards a preferential direction while in the non-poled films, many nanometric regions with random orientation exist [44]. Sencadas et al. [44] concluded that poling does not significantly affect the degree of crystallinity. Rui et al. suggested that poling fields ~ 20-30 MV/m can induce ferroelectric domains in the oriented amorphous fraction of the polymer (already mentioned as intermediate fraction which connects the crystalline lamellae and the isotropic amorphous fraction of the polymer) [54].

In this study, during the polarization of active phase particles, rotation in the PVDF chains is inevitable, increasing the number of electroactive polymorphs in the polarized films. These results are shown in the FTIR spectrum in Figure 10, in which the increase of peaks that correspond to electroactive phases is visible. The amount of PVDF electroactive phases, was ~ 70 % for non-modified NBT-BT/PVDF and APTES modified samples, while ~ 80 % was obtained for DDTES modified sample. The quantification of the electroactive phases from FTIR, has shown that the most desirable electroactive, β- phase, was found in the modified samples in the highest percentage ~ 43% (given in Table 4). Thus, besides the well-polarized active phase, the piezoelectrically active PVDF phase exists in these samples. Similar to this study, L. Ruan et al. have presented that γ- phase can be transformed into β- phase by poling at 120 °C, and the poled β- PVDF films exhibit a very strong and persistent piezoelectric effect [30].

Table 4. Percentage of electroactive phases in flexible films after polarization, output voltage obtained from finger tapping (FT) force 50 N, direct impact of the impulse hammer on the film (D) with force ~ 200 N and impulse hammer impact ~ 200 N on a metal plate (P), d_{33} and g_{33} piezoelectric coefficients obtained from high frequency measurements

SAMPLE	β	γ	F_{EA}	U (V)			d_{33}	g_{33}
	%	%	%	FT/50 N	200 N/D	200 N/P	pC/N	mVm/N
NBT-BT-APTES/PVDF	**43**	**29**	**72**	**4**	**10**	**15**	**3.32**	**11.54**
NBT-BT-DDTES/PVDF	**44**	**38**	**82**	**3**	**5**	**7.5**	**3.72**	**14.47**
NBT-BT/PVDF	**27**	**42**	**69**	**2**	**3-4**	**5**	**2.85**	**9.12**

3.2.2.5. Piezoelectric properties and Energy harvesting potential

The piezoelectric properties are displayed in Table 4. The DDTES sample has the highest value of d_{33} and g_{33} coefficients while the other two samples show slightly lower values. However, all obtained values were higher than the piezoelectric coefficient measured for the neat hot-pressed PVDF film (~ 0.2 pC/N). It is important to emphasize that these d_{33} values were measured at high frequency (~ 2 MHz) and possible differences with the values obtained from other types of measurements, like in this study, by impact hammer measurement or other quasi-static measurements, performed at ~ 1-10 Hz, are expected. It must be remarked that, although d_{33} values of composite films are smaller than for piezoelectric ceramics (e.g. 180 pC/N for NBT-BT), the g_{33} values are comparable or even higher than the bulk corresponding values (e.g. 10 mV m/N for NBT-BT), due to the smaller dielectric constant of composites. All results, obtained from different types of measurements, are presented in Table 4.

The voltage generation of the polymer composites while applying the force is presented in Figure 11 and Table 4.

The performed tests have shown that APTES-modified samples have the highest output voltage for each type of test, in comparison with the other two samples. Finger tapping has the impact localized on one small part of the sample and it gave proportionally lower values of output voltage in comparison with tests with impulse hammer. According to the FTIR results, it was expected that DDTES-modified samples, that have the highest amount of electroactive phases and d_{33} value, along with a good crystallinity degree, will give proportionally high output voltage. This was not the case possibly due to the inhomogeneous dispersion of particles in this

module. However, APTES-modified samples have shown an output voltage of up to 15 V, the highest values of output current of ~ 15 μA, and a maximum generated power of up to 225 μW. For comparison, the average power consumption of a quartz oscillator is ~ 100 nW, an electronic watch is driven with ~ 1 μW, radio frequency identification tags work with ~ 10 μW of power, while hearing aids and remotes need ~ 100 μW, etc [64, 65]. Therefore, the harvesters prepared in this study are good candidates for low-power portable electronic systems and self-powered sensing devices.

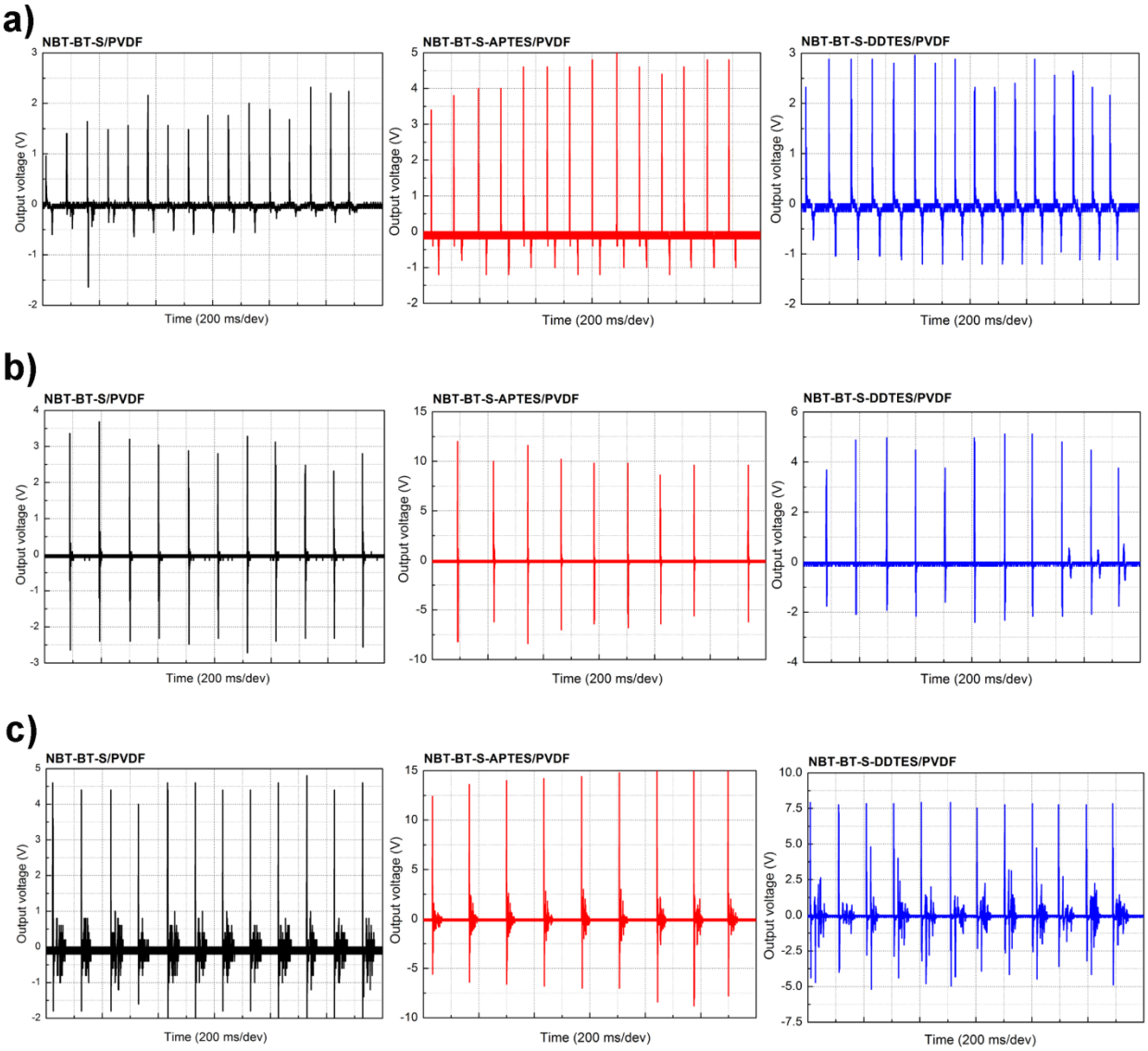

Figure 11. Output voltage obtained for the samples a) finger tapping ~ 50 N, b) under the direct impact of the impulse hammer with rubber end ~ 200 N and c) under the impact of impulse hammer on the metal plate placed above the sample ~ 200 N

4. Conclusions

The main goal of this work was to study the effect of surface modification inorganic ferroelectric particles on the structure and properties of composite flexible films prepared by mixing the inorganic powder with PVDF polymer. Surface modification of filler particles was performed by two different coupling agents, polar APTES and non-polar DDTES. It was found that each coupling agent differently affects the structure and properties of the produced flexible films due to the formation of bonds (that differ in charge and nature) between their respective functional groups and PVDF polymer chains. Modification of filler particles with coupling agents increased the percentage of electroactive PVDF polymorphs in the films up to 67% (before polarization). In the APTES samples, 52 % of electroactive β-phase was detected; its higher polarity enhanced the interaction with the PVDF chains. The dielectric permittivity values were lower in modified samples due to tailored interfaces between particles and polymer. The ferroelectric loops had similar shapes but the APTES-modified films were able to withstand higher applied fields due to more homogeneous distribution of filler particles in the polymer. The DDTES layer apparently can block the branching of conductive paths but structural defects have a dominant effect and direct contact between particles forms a pathway for conduction charges, leading to a deterioration of the breakdown strength. Moreover, the amorphous part of the APTES-modified samples possibly possesses more mobile amorphous fractions that enable the formation of ferroelectric domains and enhance the ferroelectric properties of this film.

The polarization of the films enabled the formation of electroactive β- phase in modified samples. Piezoelectric charge coefficients, $d_{33,}$ and piezoelectric voltage coefficients, g_{33}, obtained from measurements at 2 MHz, were higher than for non-modified material. Up to 15 V of output voltage was obtained for APTES-modified samples by testing with impulse hammer load thanks to the formation of a high concentration of polar PVDF phases and proper bonding of NBT-BT particles with the PVDF chains.

The final conclusion that can be drawn out from this study is that surface modification of filler particles, especially by silanization with an APTES coupling agent, is a useful method for improving the polymer-particle interface development. In this way, it is possible to improve filler compatibility and connectivity with PVDF polymer chains, increase the breakdown strength of the material, and finally enhance the functional properties of the piezoelectric module. The maximum power obtained from this single module is 225 μW, which is enough for powering up

many sensors, low power microcontrollers, alarms, LED lights, and other low-power and ultra-low power devices which make these composites interesting for energy harvesting applications.

Acknowledgement

The authors gratefully acknowledge the Ministry of Science, Technological Development and Innovations of the Republic of Serbia for financial support given through national programs (project code 451-03-47/2023-01/200053 and 451-03-47/2023-01/200103) and bilateral project (project code in SR 451-03-03064/2018-09/1) “Lead-free piezoelectric and multiferroic flexible films for nanoelectronics and energy harvesting” with Italy and Ministry of Foreign Affairs and International Cooperation of Italy (project code: RS19MO01). Dr Ivan Stijepovic from the Faculty of Technology, University of Novi Sad for the XRD analysis of films is gratefully acknowledged. Floriana Craciun and Francesco Cordero thank Massimiliano Latino from CNR-ISM for technical assistance.

Conflict of Interest Statement

The authors declare that they have no known competing financial interests or personal relationships that could have appeared to influence the work reported in this paper.

Reference

[1] Y. Lu, J. Chen, Z. Cheng, S. Zhang, The PZT/Ni unimorph magnetoelectric energy harvester for wireless sensing applications, Energ. Convers. Manage. 200 (2019) 112084
DOI: https://doi.org/10.1016/j.enconman.2019.112084

[2] J. D. Bobic, G. Ferreira Teixeira, R. Grigalaitis, S. Gyergyek, M. M. Vijatović Petrovic, M. Ap. Zaghete, B. D. Stojanovic, PZT–NZF/CF ferrite flexible thick films: Structural, dielectric, ferroelectric, and magnetic characterization. J. Adv. Ceram. 8 (4) (2019) 545–554
DOI: https://doi.org/10.1007/s40145-019-0337-1

[3] A.K. Sharma, J.K. Swamy, A. Jain, Dielectric properties of PVDF-PZT composite films and their thermal dependence. Adv. Mater. Proceedings 1(2) (2016) 185-190
DOI: 10.5185/amp.2016/213

[4] D.P. Anh, D.V. On, D.A. Quang, N. Van Thinh, N. T. Anh Tuyet, V. Thanh Tung, T. Van Chuong, Dielectric and Piezoelectric Properties of PZT/PVDF Composites Prepared by Hot Press Method, Inter. J. Engin. Res. Technol. 9 (4) (2020) 898-902 DOI: 10.17577/IJERTV9IS040586

[5] B. Li, Q. Liu, X. Tang, T. Zhang, Y. Jiang, W. Li, J. Luo, High Energy Storage Density and Impedance Response of PLZT2/95/5 Antiferroelectric Ceramics, Materials 10 (2017) 143 DOI: https://doi.org/10.3390/ma10020143

[6] A. Jain, K.J. Prashanth, A. Kr. Sharma, A. Jain, P.N. Rashmi, Dielectric and Piezoelectric Properties of PVDF/PZT Composites: A Review, Polym. Eng. Sci. 55(7) (2015) 1589-1616 DOI: https://doi.org/10.1002/pen.24088

[7] J. Wu, Perovskite lead-free piezoelectric ceramics, J Appl Phys, 127 (2020) 190901 DOI 10.1063/5.0006261

[8] J. Zhang, Y. Lin, L. Wang, Y. Yang, H. Yang, Q. Yuan, Significantly enhanced energy storage density in sodium bismuth titanate-based ferroelectrics under low electric fields, J. Eur. Ceram. Soc. 40 (15) (2020) 5458-5465 DOI 10.1016/j.jeurceramsoc.2020.06.059

[9] S. Mishra, L. Unnikrishnan, S.K. Nayak, S. Mohanty, Advances in piezoelectric polymer composites for energy harvesting application: A Systematic review , Macromol. Mater. Eng. 304 (2019)1800463 DOI: https://doi.org/10.1002/mame.201800463

[10] S.K. Sharma, H. Gaur, M. Kulkarni, G. Patil, B. Bhattacharya, A. Sharma, PZT–PDMS composite for active damping of vibrations, Compos. Sci. Technol. 77 (2013) 42–51 DOI: https://doi.org/10.1016/j.compscitech.2013.01.004

[11] M. Vijatovic Petrovic, F. Cordero, E. Mercadelli, E. Brunengo, N. Ilic, C. Galassi, Z. Despotovic, J. Bobic, A. Dzunuzovic, P. Stagnaro, G. Canu, F. Craciun, Flexible lead-free NBT-BT/PVDF composite films by hot pressing for low- energy harvesting and storage J. Alloy. Compd. 884 (2021) 161071 DOI: https://doi.org/10.1016/j.jallcom.2021.161071

[12] F. Craciun, F. Cordero, E. Mercadelli, N. Ilic, C. Galassi, C. Baldisserri, J. Bobic, P. Stagnaro, G. Canu, M. Teresa Buscaglia A. Dzunuzovic, M. Vijatovic Petrovic, Flexible composite films with enhanced piezoelectric properties for energy harvesting and wireless ultrasound-powered technology, Composites Part B, 236 (2023) 110835 DOI: https://doi.org/10.1016/j.compositesb.2023.110835

[13] J. D. Bobic, N. Ilic , Z. Despotovic, A. Dzunuzovic, R. Grigalaitis, I. Stijepovic, B. Stojanovic, M. Vijatovic Petrovic, Properties and Potential Application of Lead-Free (BaZr0.2Ti0.8O3) and Lead-Based (PbZr0.52Ti0.48O3) Flexible Thick Films, Crystals 13 (2023) 1178 DOI: https://doi.org/10.3390/cryst13081178

[14] T. Vijayakanth, D.J. Liptrot, E. Gazit, R. Boomishankar, C.R. Bowen, Recent Advances in Organic and Organic–Inorganic Hybrid, Materials for Piezoelectric Mechanical Energy Harvesting, Adv. Funct. Mater. 2022, 2109492 DOI: https://doi.org/10.1002/adfm.202109492

[15] S. Requena, S. Lacoul, Y.M. Strzhemechny, Luminescent Properties of Surface Functionalized $BaTiO_3$ Embedded in Poly(methyl methacrylate), Materials 7 (2014) 471-483 DOI: https://doi.org/10.3390/ma7010471

[16] R. Prateek, S. Bhunia, A. Siddiqui, R. Garg, G. Kumar, Significantly Enhanced Energy Density by Tailoring the Interface in Hierarchically Structured TiO_2−$BaTiO_3$−TiO_2 Nanofillers in PVDF Based Thin-Film Polymer Nanocomposites, ACS Appl. Mater. Interfaces 11 (2019) 14329−14339 DOI: https://doi.org/10.1021/acsami.9b01359

[17] M. V.Silibin, A. V.Solnyshkin, D. A.Kiselev, A. N. Morozovska, E. A. Eliseev, S. A. Gavrilov, M. D. Malinkovich, D. C. Lupascu, V. V. Shvartsman, Local ferroelectric properties in polyvinylidene fluoride/barium lead zirconate titanate nanocomposites: Interface effect, J. Appl. Phys. 114 (2013) 144102 DOI: https://doi.org/10.1063/1.4824463

[18] H. Luo, X. Zhou, C. Ellingford, Y. Zhang, S. Chen, K. Zhou, D. Zhang, C.R. Bowen, C. Wan, Interface design for high energy density polymer nanocomposites, Chem. Soc. Rev. 48 (2019) 4424 DOI: 10.1039/C9CS00043G

[19] N. Meng, X. Zhu, R. Mao, M. J.Reece, E. Bilotti, Nanoscale interfacial electroactivity in PVDF/PVDF-TrFE blended films with enhanced dielectric and ferroelectric properties, J. Mater. Chem. C, 5 (2017) 3296 DOI: https://doi.org/10.1039/C7TC00162B

[20] X. Bi, L. Yang, Z. Wang, Y. Zhan, S. Wang, C. Zhang, Y. Li, Y. Miao, J. Zha, Construction of a Three-Dimensional $BaTiO_3$ Network for Enhanced Permittivity and Energy Storage of PVDF Composites, Materials 14 (2021) 3585 DOI: https://doi.org/10.3390/ma14133585

[21] Z. Dang, H. Wang, H. Xu, Influence of silane coupling agent on morphology and dielectric property in $BaTiO_3$/polyvinylidene fluoride composites, Appl. Phys. Lett., 89 (2006) 112902 DOI: https://doi.org/10.1063/1.2338529

[22] A.M. Chandran, P. Kumar, S. Mural, Surface silanized MWCNTs doped PVDF nanocomposite with self-organized dipoles: an intrinsic study on the dielectric, piezoelectric, ferroelectric, and energy harvesting phenomenology, Sustain. Energ. Fuels, 6 (2022) 1641 DOI: https://doi.org/10.1039/D1SE01256H

[23] T. Tuyet Mai Phan, N. Chau Chu, V. Boi Luu, H. Nguyen Xuan, D. Thang Pham, I. Martin, P. Carriere, Enhancement of polarization property of silane-modified $BaTiO_3$ nanoparticles and its effect in increasing dielectric property of epoxy/$BaTiO_3$ nanocomposites, J. Sci.: Adv. Mater. Dev. 1 (2016) 90-97 DOI: https://doi.org/10.1016/j.jsamd.2016.04.005

[24] D. S. Nakonieczny, F. Kern , L. Dufner, A. Dubiel, M. Antonowicz, K. Matus , Effect of Calcination Temperature on the Phase Composition, Morphology, and Thermal Properties of ZrO_2 and Al_2O_3 Modified with APTES (3-aminopropyltriethoxysilane), Materials 14 (2021) 6651 DOI: https://doi.org/10.3390/ma14216651

[25] A. Lucia, M. Bacher, H.W. G. van Herwijnen, T. Rosenau, A Direct Silanization Protocol for Di-aldehyde Cellulose, Molecules 25 (2020) 2458 DOI: https://doi.org/10.3390/molecules25102458

[26] C. Min, P. Nie, D. Shen, K. Zhao, X. Chen, Preparation and Electrical Properties of PLZT/PVDF Nanocomposites, J. Polym. Mater. 31 (2014) 199-209

[27] R. Li, L. Zhang, Z. Shi, J. Pei, Effects of Coupling Agents on the Structure and Electrical Properties of PZT-Poly(Vinylidene Fluoride) Composites, Appl. Sci. 6 (2016) 282 DOI: https://doi.org/10.3390/app6100282

[28] M. Castellano, L. Conzatti, G. Costa, L. Falqui, A. Turturro, B. Valenti, F. Negroni, Surface modification of silica: 1. Thermodynamic aspects and effect on elastomer reinforcement, Polymer 46 (2005) 695. DOI: https://doi.org/10.1016/j.polymer.2004.11.010

[29] T. Takenaka, K. Maruyama, K. Sakata, $(Bi_{1/2}Na_{1/2})TiO_3$-$BaTiO_3$ System for lead-free piezoelectric ceramics, Jpn. J. Appl. Phys. 30 (1991) 2236–2239 DOI: 10.1143/JJAP.30.2236

[30] L. Ruan, X. Yao, Y. Chang, L. Zhou, G. Qin, X. Zhang, Properties and Applications of the β Phase Poly(vinylidene fluoride), Polymers 10 (2018) 228 DOI: https://doi.org/10.3390/polym10030228

[31] P. Martins, A.C. Lopes, S. Lanceros-Mendez, Electroactive phases of poly(vinylidene fluoride): Determination, processing and applications, Prog. Polym. Sci. 39 (2014) 683–706 DOI: https://doi.org/10.1016/j.progpolymsci.2013.07.006

[32] H.-J. Ye, L. Yang, W.-Z. Shao, S.-B. Sun, L. Zhen, Effect of electroactive phase transformation on electron structure and dielectric properties of uniaxial stretching poly(vinylidene fluoride) films, RSC Adv. 3 (2013) 23730–23736 DOI: https://doi.org/10.1039/C3RA43966F

[33] L. Yang, J. Qiu, K. Zhu, H. Ji, Q. Zhao, M. Shen, S. Zeng, Effect of rolling temperature on the microstructure and electric properties of β-polyvinylidene fluoride films, J. Mater. Sci. Mater. Electron. 29 (2018) 15957–15965 DOI: https://doi.org/10.1007/s10854-018-9681-0

[34] X. Cai, T. Lei, D. Sun, L. Lin, A critical analysis of the α, β and γ phases in poly(vinylidene fluoride) using FTIR, RSC Adv. 7 (2017) 15382–15389 DOI: https://doi.org/10.1039/C7RA01267E

[35] A.M. Chandran, S. Varun, S. Cherumannil Karumuthil, S. Varghese, P. Kumar S. Mural, Zinc Oxide Nanoparticles Coated with (3-Aminopropyl)triethoxysilane as Additives for Boosting the Dielectric, Ferroelectric, and Piezoelectric Properties of Poly(vinylidene fluoride) Films for Energy Harvesting, ACS Appl. Nano Mater. 4 (2021) 1798−1809 DOI: https://doi.org/10.1021/acsanm.0c03214

[36] S. Dalle Vacche, F. Oliveira, Y. Leterrier, V. Michaud, D. Damjanovic, J.-Anders E. Manson, Effect of silane coupling agent on the morphology, structure and properties of poly(vinylidene fluoride–trifluoroethylene)/$BaTiO_3$ composites, J. Mater. Sci. 49 (2014) 4552–4564 DOI: https://doi.org/10.1007/s10853-014-8155-x

[37] R. Gregorio, Jr., Determination of the α, β, and γ Crystalline Phases of Poly(vinylidene fluoride) Films Prepared at Different Conditions, J. Appl. Poly. Sci. 100 (2006) 3272–3279 DOI: https://doi.org/10.1002/app.23137

[38] R. Gregorio, E.M. Ueno, Effect of crystalline phase, orientation and temperature on the dielectric properties of poly(vinyli-dene fluoride) (PVDF), J. Mater. Sci. 34 (1999) 4489–500 DOI: https://doi.org/10.1023/A:1004689205706

[39] S. Prasanna Muduli, S. Parida , S.K. Rout, S. Rajput, M. Kar, Effect of hot press temperature on β-phase, dielectric and ferroelectric properties of solvent casted Poly(vinyledene fluoride) films, Mater. Res. Express 6 (2019) 095306 DOI: 10.1088/2053-1591/ab2d85

[40] E. Brunengo, L. Conzatti, I. Schizzi, M. Teresa Buscaglia, G. Canu, L. Curecheriu, C. Costa, M. Castellano, L. Mitoseriu, P. Stagnaro, V. Buscaglia, Improved dielectric properties of

poly(vinylidene fluoride)–$BaTiO_3$ composites by solvent-free processing J. Appl. Polym. Sci. 138(12) (2020) e50049 DOI: https://doi.org/10.1002/app.50049

[41] M. Kubin, P. Makreski, M. Zanoni, G. Selleri, L. Gasperini, D. Fabiani, C. Gualandi, A. Buzarovska, Piezoelectric properties of PVDF-TrFE/BaTiO3 composite foams with different contents of TrFE units, Polymer Composites. 44 (2023) 7804-7816 DOI:10.1002/pc.27667

[42] W. Xia, Z. Zhang, PVDF-based dielectric polymers and their application in electronic materials, IET Nanodielectrics Rev. 1 (2018) 17-31 DOI: https://doi.org/10.1049/iet-nde.2018.0001

[43] Y. Fu, Y. Wang, S. Wang, Z. Gao, C. Xiong,Enhanced Breakdown Strength and Energy Storage of PVDF-based Dielectric Composites by Incorporating Exfoliated Mica Nanosheets, Polym. Compos. 40 [5] (2019) 2088-2094 DOI: https://doi.org/10.1002/pc.24991

[44] V. Sencadas, C.M. Costa, V. Moreira, J. Monteiro, S.K. Mendiratta, J.F. Mano, S. Lanceros-Méndez, Poling of β-poly(vinylidene fluoride): dielectric and IR spectroscopy studies, e-Polymers 2005; 002 DOI: https://doi.org/10.1515/epoly.2005.5.1.10.

[45] P. Mao, J. Wang, L. Zhang, Q. Sun, X. Liu, L. He, S. Liu, S. Zhang, H. Gong, Tunable dielectric polarization and breakdown behavior for high energy storage capability in P(VDF–TrFE–CFE)/PVDF polymer blended composite films, Phys. Chem. Chem. Phys. 22 (2020) 13143 DOI: https://doi.org/10.1039/D0CP01071E

[46] M. Samet, A. Kallel, A. Serghei, Maxwell-Wagner-Sillars interfacial polarization in dielectric spectra of composite materials: Scaling laws and applications, J. Compos. Mater. 56 (2022) 3197–3217 DOI: https://doi.org/10.1177/00219983221090629

[47] D. Shen, Q. Zhang, Z. Zhang, H. Yang, J. Sheng, Enhanced Dielectric and Hydrophobic Properties of Poly(vinylidene fluoride-trifluoroethylene)/TiO_2 Nanowire Arrays Composite Film Surface Modified by Electrospinning, Polymers 13 (2021) 105 DOI: https://doi.org/10.3390/polym13010105

[48] Y. Li, J. Ho, J. Wang, Z.-Ming Li, G.-Ji Zhong, L. Zhu, Understanding Nonlinear Dielectric Properties in a Biaxially Oriented Poly(vinylidene fluoride) Film at Both Low and High Electric Fields, ACS Appl. Mater. Interfaces 8 (2016) 455−465 DOI: https://doi.org/10.1021/acsami.5b09368

[49] G. Rui, E. Allahyarov, J.J. Thomas, P.L. Taylor, L. Zhu, Temperature-Dependent Rotational Dipole Mobility and Devitrification of the Rigid Amorphous Fraction in Unpoled and Poled Biaxially Oriented Poly(vinylidene fluoride), Macromolecules 55 (2022) 9705−9714 DOI: https://doi.org/10.1021/acs.macromol.2c01110

[50] Y. Jiang, Z. Zhang, Z. Zhou, H. Yang, Q. Zhang, Enhanced Dielectric Performance of P(VDF-HFP) Composites with Satellite–Core-Structured Fe2O3@BaTiO3 Nanofillers, Polymers 11(2019) 1541 DOI: https://doi.org/10.3390/polym11101541

[51] H.S. Mohanty, Ravikant, A. Kumar, P.K. Kulriya, R. Thomas, D.K. Pradhan, Dielectric/ferroelectric properties of ferroelectric ceramic dispersed poly(vinylidene fluoride) with enhanced β-phase formation, Mater. Chem. Phys. 230 (2019) 221-230 DOI: https://doi.org/10.1016/j.matchemphys.2019.03.055

[52] Y. Wang, M. Yao, R. Ma, Q. Yuan, D. Yang, B. Cui, C. Ma, M. Liu, D. Hu, Design strategy of barium titanate/polyvinylidene fluoride-based nanocomposite films for high energy storage, J. Mater. Chem. A 8 (2020) 884-917 DOI: https://doi.org/10.1039/C9TA11527G

[53] H. Luo, D. Zhang, C. Jiang, X. Yuan, C. Chen, K. Zhou, Improved dielectric properties and energy storage density of Poly(vinylidene fluoride-co-hexafluoropropylene) nanocomposite with Hydration epoxy resin coated $BaTiO_3$, ACS Appl. Mater. Inter. 7 (2015) 8061-8069 DOI: https://doi.org/10.1021/acsami.5b00555

[54] G. Rui, Y. Huang, X. Chen, R. Li, D. Wang, T. Miyoshid, L. Zhu, Giant spontaneous polarization for enhanced ferroelectric properties of biaxially oriented poly(vinylidene fluoride) by mobile oriented amorphous fractions, J. Mater. Chem. C 9 (2021) 894 DOI: https://doi.org/10.1039/D0TC04632A

[55] Q. Cao, W. Zhu, W. Chen, X. Chen, R. Yang, S. Yang, H. Zhang, X. Gui, J. Chen, Nonsolid TiOx Nanoparticles/PVDF Nanocomposite for Improved, Energy Storage Performance, ACS Appl. Mater. Interfaces 14 (2022) 8226−8234 DOI: https://doi.org/10.1021/acsami.1c18544

[56] F. Pedroli, A. Flocchini, A. Marrani, M.-Quyen Le, O. Sanseau, P.-Jean Cottinet, J.-Fabien Capsal, Boosted energy-storage efficiency by controlling conduction loss of multilayered polymeric capacitors, Mater. Design 192 (2020) 108712 DOI: https://doi.org/10.1016/j.matdes.2020.108712

[57] J. Wang, Z.-Hui Shen, Modeling-guided understanding microstructure effects in energy storage dielectrics, Microstructures 1 (2021) 2021006 DOI: 10.20517/microstructures.2021.05

[58] Y. Yu, X.-Ming Wang, De-Chao Bu, Y. Feng, M.-He Chi, Influence of spinel ZnMn2O4 particles on the dielectric performance of PVDF-based composites, Polymer Composites. 43 (2022) 8715–8724 DOI: https://doi.org/10.1002/pc.27052

[59] Y. Chen, W. Zhu, X.Wang, W. Chen, W. Cai, Z. Xiao, J. Chen, Improving the comprehensive energy storage performance of composite materials through the coupling effect of AgNbO3/PVDF nanocomposite, Polym. Compos. 43 [8] (2022) 5250 DOI: https://doi.org/10.1002/pc.26818

[60] G. Ho Kim, S. Man Hong, Y. Seo, Piezoelectric properties of poly(vinylidene fluoride) and carbon nanotube blends: β-phase development, Phys. Chem. Chem. Phys. 11 (2009) 10506–10512 DOI: https://doi.org/10.1039/B912801H

[61] Y. Jiang, Y. Ye, J. Yu, Z. Wu, W. Li, J. Xu, G. Xie1, Study of Thermally Poled and Corona Charged Poly(vinylidene fluoride) Films, Polym. Eng Sci, 47 [9] (2007) 1344-1350 DOI: https://doi.org/10.1002/pen.20817

[62] A. Hartono, Darwin, Ramli, Suparno Satira, Mitra Djamal,Herman, Electric Field Poling 2GV/m to Improve Piezoelectricity of PVDF Thin Film, AIP Conference Proceedings 1719 (2016) 030021 DOI: https://doi.org/10.1063/1.4943716

[63] P. Ueberschlag, PVDF piezoelectric polymer, Sensor Review, 21 (2001) 118-125 DOI: https://doi.org/10.1108/02602280110388315

[64] M. T. Todaro, F. Guido, L. Algieri, V.M. Mastronardi, D. Desma¨ele, G. Epifani, M. De Vittorio, Biocompatible, Flexible, and Compliant Energy Harvesters Based on Piezoelectric Thin Films, IEEE T Nanotechnol. 17 (2018) 220-230 DOI: 10.1109/TNANO.2017.2789300

[65] V. Annapureddy, H. Palneedi, G.-Tae Hwang, M. Peddigari, D.-Yong Jeong, W.-Ha Yoon, K.-Ho Kim, J. Ryu, Magnetic energy harvesting with magnetoelectrics: an emerging technology for self-powered autonomous systems, Sustain. Energ. Fuels, 1 (2017) 2039 DOI: https://doi.org/10.1039/C7SE00403F